Facies analysis, foraminiferal record and chronostratigraphy of Holocene sequences from Saltés Island (Tinto-Odiel estuary, SW Spain): The origin of high-energy deposits

M.L. González-Regalado[a], P. Gómez[a], F. Ruiz[a,f,*], L.M. Cáceres[a], M.J. Clemente[a], J. Rodríguez Vidal[a], A. Toscano[a], G. Monge[b], M. Abad[c], T. Izquierdo[c], J.M. Campos[d], J. Bermejo[d], A. Martínez-Aguirre[e], M.I. Prudencio[f], M.I. Dias[f], R. Marques[f], J.M. Muñoz[g]

[a] *Departamento de Ciencias de la Tierra, Universidad de Huelva, Avda. Tres de Marzo s/n, 21071, Huelva, Spain*
[b] *Departamento de Cristalografía, Mineralogía y Química Agrícola, Universidad de Sevilla, 41071, Sevilla, Spain*
[c] *Departamento de Geología, Facultad de Ingeniería, Universidad de Atacama, Avda. Copayapu 485, Copiapó, Chile*
[d] *Departamento de Historia I, Universidad de Huelva, Avda. Tres de Marzo s/n, 21071, Huelva, Spain*
[e] *Departamento de Física Aplicada I, EUITA, Universidad de Sevilla, Crta. Utrera km 1, 41013, Sevilla, Spain*
[f] *Centro de Ciências e Tecnologias Nucleares (C2TN), Instituto Superior Técnico, Universidade de Lisboa, Estrada Nacional 10 (km 139.7), 2695-066, Bobadela LRS, Portugal*
[g] *Departamento de Estadística e Investigación Operativa, Universidad de Sevilla, Avda. Reina Mercedes, s/n, 41012, Sevilla, Spain*

Keywords:
Palaeoenviromental reconstruction. Washover fan. Chenier. Holocene. SW Spain

A B S T R A C T

A multidisciplinary analysis of Holocene sediments from La Cascajera (Tinto-Odiel estuary, SW Spain) has allowed to differentiate five sedimentary facies (sandy tidal flat, clayey tidal flat, washover fan, salt marsh, edaphic horizon), according to their granulometric characteristics, internal structure, mineralogical composition, clay mineral assemblage and paleontological record. These data, coupled to ^{14}C AMS dating, suggest an evolution from a sandy tidal plain to a chenier before 2100 cal yr BP. This initial chenier was partially eroded later by regional storms between 2100 cal yr BP and 1900 cal yr BP, leading to the deposition of two washover fans. These facies have been eroded in the last centuries by the action of an ebb-tide channel.

1. Introduction

In coastal areas, numerous studies have recently been focused on the historical or geological record of high-energy events such as storms, tsunamis, cyclones or hurricanes, in order to understand their temporal cyclicity (Donnelly et al., 2004; Benoit et al., 2007; Nikitina et al., 2014; Bregy et al., 2018). Other investigations have also tried to differentiate through multidisciplinary studies the characteristics of deposits derived from tsunamis or storms (Morton et al., 2007; Lario et al., 2010; Ramírez-Herrera et al., 2012; Schneider et al., in press). Washover fans and cheniers are some of these deposits.

Washover fans (*sensu* Price, 1947) are resultant backshore deposits derived from these overwash phenomena in lakes and coastal areas (Davidson and Fisher, 1992; Duck and Da Silva, 2012; Granier and Boichard, 2017). These high-energy deposits are due to hurricanes (Rodríguez et al., 2013; Braun et al., 2017), typhoons (Brill et al., 2016), cyclones (May et al., 2017), storms (Clemmensen et al., 2016), tsunamis (Clague et al., 1994; Willershauser et al., 2015) or even sea-level changes (Miguel et al., in press).

The resulting stratigraphic beds have been reviewed and modeled, with a wide geomorphological range (length: 10 m-5 km; thickness: 10 cm-5 m) (Schwartz, 1982; Sedgwick and Davis, 2003; Hudock et al., 2014). The final morphological and structural responses to all these phenomena depend on numerous factors, such as the wave heigths and duration of the events, constructive and destructive interferences of induced waves, variations in nearshore bathymetry or the previous coastal geomorphology of the affected areas (Morton and Sallenger, 2003; Phantuwongraj et al., 2013).

The macropalaeontological record of washover fans is one of the most interesting characteristics to determine them and to infer the origin of these deposits. One of the most frequent features is the presence of numerous shelly layers with bivalves, gastropods and even fragments of corals (Sabatier, 2009; Ledesma-Vázquez et al., 2007; Switzer et al., 2011; Gutiérrez-Más, 2011). On the other hand,

* Corresponding author. Departamento de Ciencias de la Tierra, Universidad de Huelva, Avda. Tres de Marzo s/n, 21071, Huelva, Spain. Tel.: +34 959219850.
E-mail address: ruizmu@uhu.es (F. Ruiz).

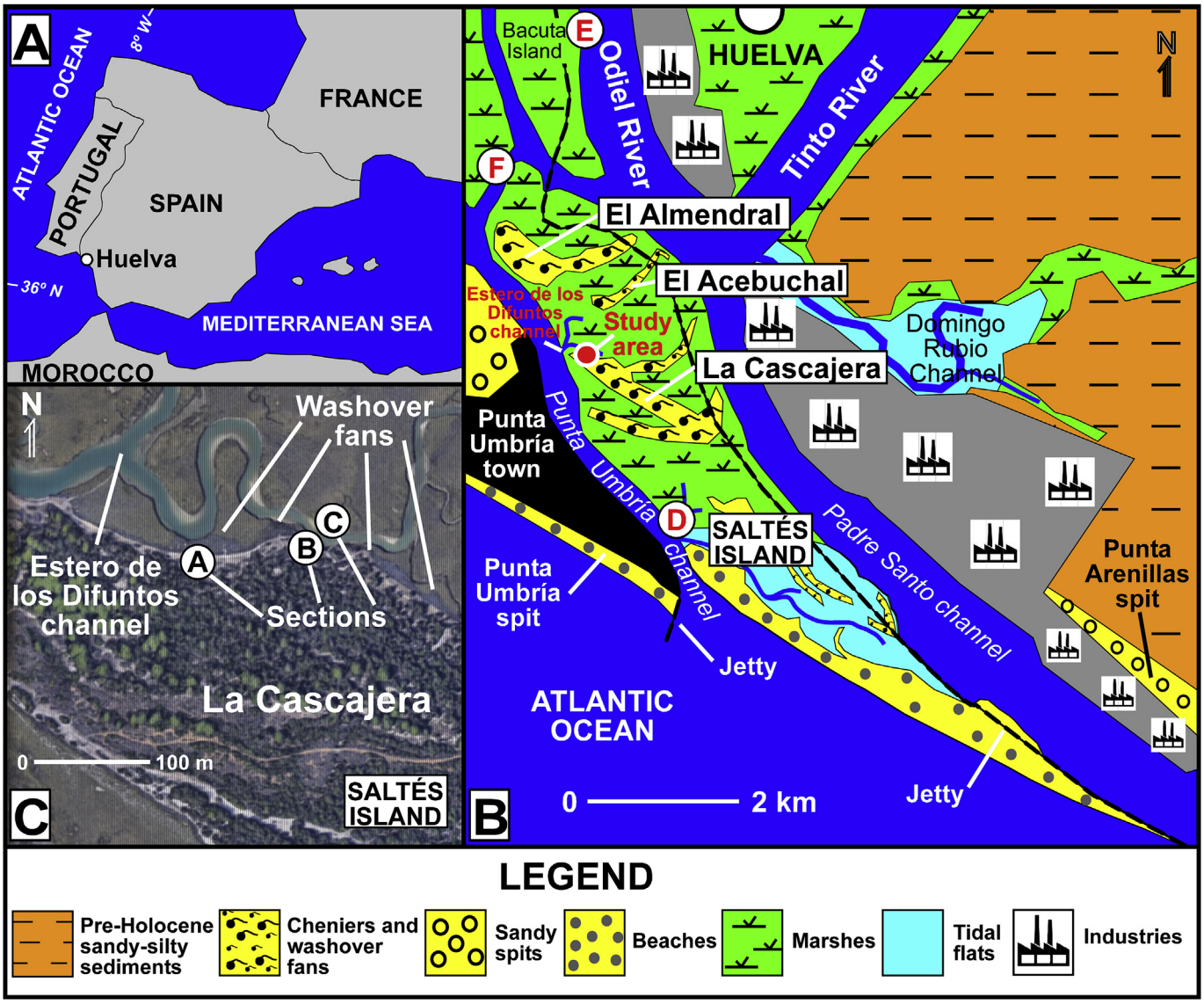

Fig. 1. A: Location map; B: Marine domain of the Tinto-Odiel estuary: main geomorphological features and location of the study area, the extracted drill core (D) and the two surface samples (E and F); C: location of the studied sections, the northern washover fans of La Cascajera chenier and the Estero de los Difuntos channel.

washover fans are environments that cause stratigraphical and ecological changes in coastal ecosystems, with interesting ichnological consequences (Martin and Rindsberg, 2011).

This palaeontological analysis is usually completed with the study of the vertical distribution of microfossils. In most cases, this additional research is focused on the foraminiferal assemblages (e.g. Hippensteel and Martin, 2000; Hippensteeel et al., 2013; Brill et al., 2016). Ostracods, diatoms or pollen can also contribute to the identification of these high-energy deposits (Costas et al., 2009; Ruiz et al., 2010; Pilarczyk et al., 2014; Gomes et al., 2017).

This multi-proxy differentiation is very important to determine the periods of recurrence of these phenomena (Monecke et al., 2008; Erikson et al., 2018; Fuller et al., 2018). In addition, it is a critical issue in coastal assessment (González et al., 2009; Atwater et al., 2012) and the development of risk maps and the associated economic, equitable and affordable adaptations (Wainwright et al., 2015; Fletcher et al., 2016; Pile et al., 2018).

Cheniers are coastal, wave-built ridges composed of sands, gravels and bioclastic components deposited on muddy tidal flats (Otvos and Price, 1979). In most cases, these ridges can be formed by littoral drifts or by wave-winowing of muddy sediments and concentration of coarse particles (Augustinus, 1989). Two o more cheniers separated by muddy flats constitute a chenier plain (Otvos and Price, 1979).

In this paper, we conducted a granulometric, stratigraphic, mineralogical and palaeontological analysis of washover fans and cheniers identified on Saltés Island (Tinto-Odiel estuary, SW Spain). The palaeontological record is compared to that of different adjacent environments in order to deduce the origin of these deposits, while the record of high-energy events are revised to infer the hydrodynamic scenarios that produced them.

2. Study area

2.1. Holocene evolution of southwestern Spain: tsunamis, storms and sea level

In southwestern Spain, numerous multidisciplinary studies have focused on the Holocene evolution of estuaries, sea level changes, high-energy events and its associated deposits (e.g. washover fans, among others). According to them, the Flandrian transgressive maximum took place at 6450 ^{14}C years BP (Dabrio et al., 1995; Goy et al., 1996). Four phases of progradation have been delimitated, separated by erosive

periods: H_1 (6500–4700 cal. BP), H_2 (4400–2700 cal. BP), H_3 (2400–700 cal. BP) and H_4 (500 cal. BP-present) (Goy et al., 1998; Borja et al., 1999). Nevertheless, recent research indicates that sea level has continued to rise from 4 ka to present in coastal areas of the Iberian Peninsula (0.1 ± 0.5 mm yr^{-1}; García-Artolas et al., 2017).

This area is a low-probability tsunamigenic zone, but its geological and archaeological records include evidence of more than dozen tsunamis that have ravaged these coasts and the adjacent Portuguese littoral during the last thousands of years, according to historical data (Galbis, 1932, 1940). They include chenier-like ridges or washover fans (for a review, see Ruiz et al., 2013), most of them derived from the 218-210 BC or 1755 AD tsunamis (e.g. Ruiz et al., 2005; Lario et al., 2011; Rodríguez Vidal et al., 2011, a; b; Font et al., 2013).

In addition, winter storms periodically cause significant damage or changes to beaches (erosion, washover fan deposits, changes in ecosystems), port structures, boardwalks and even cause the loss of human life. The most destructive storms (wave height > 6 m; wind speed > 115 km/h) cause losses even higher than 12 M€ per year, with a long cycle of 6–7 years preceding a short subsequent cycle of 2–3 years according to studies conducted between 1960 and 1996 (Ruiz et al., 2005b), but new studies are needed that include historical periods and the last two decades. Consequently, it is necessary to define the main characteristics of the storm and tsunamigenic deposits in this area, in order to model their recurrence periods, the coastal areas susceptible to be affected and the associated risk maps.

2.2. The Tinto-Odiel estuary

The Tinto-Odiel Estuary is a 25-km-long incised valley on the southwestern coast of Spain, underlaying by pre-Holocene sandy-silty sediments (Fig. 1A–B). The marine domain is characterized by: a) marsh (Fig. 1B: Bacuta Island) in which vegetation is dominated by species tolerant of variable salinity such as *Sarcocornia fruticosa* and *Spartina densiflora* (Rubio, 1985); b) barrier islands (Fig. 1B: Saltés Island) that include recurved sandy and shelly ridges (El Almendral, El Acebuchal, La Cascajera); and c) sandy spits (Fig. 1B: Punta Umbría, Punta Arenillas). A long jetty was built in 1979 at the entrance of the estuary in order to prevent the silting of the dredged ship channel, causing the creation of a new beach attached to its western face (Fig. 1B). The adjacent continental shelf is a large shoal area with very flat bottom topography gently seaward-sloping (Ojeda, 1988).

The hydrodynamics of this estuary is controlled by tides and fluvial discharges. The tidal regime is mesotidal (mean range 2.15 m) and semidiurnal, with a low diurnal amplitude (Borrego et al., 1993). Both rivers have seasonal, limited flows. The highest runoff occurs from December to February in both streams (an average of 100 hm^3/month) and the least amount of runoff takes place during the summer months (< 1 hm^3/month) (Borrego, 1992; Pendón, 1999).

2.3. The Saltés Island: La Cascajera ridge

Saltés Island occupies the central part of the estuary of the Tinto and Odiel rivers, with an elongated shape in a NW-SE direction (Fig. 1B). It is composed of a set of cheniers and washover fans (El Almendral, El Acebuchal, La Cascajera) arranged on muddy-sandy tidal flats and salt marshes, with an elevation between 0.5 m (El Acebuchal) and more than 3 m (La Cascajera) above mean sea level. Consequently, these cheniers compose a chenier plain, according to Morales et al. (2014).

La Cascajera ridge owes its name to the great abundance of *Glycymeris* shells on its surface (locally so-called ´cascajos'). It presents a hook morphology, with a complex internal structure composed of different sandy-shelly ridges of different ages and separated by marshes. Datings of bivalve shells collected from the central NW-SE ridge (Table 1) revealed calibrated ages between 2750 cal. yr. BP and 2300 cal. yr. BP for this sedimentary bed, whereas the one located in the southern sector is much more recent (1240 cal. yr. AD-710 cal. yr. AD; Dabrio et al., 2000).

The present study is focused on the northern part of this ridge. This area presents a set of washover fans (Fig. 1C) that has been partially eroded by the Estero de los Difuntos ebb-tide channel and several sections (Fig. 1C: A-B-C) are now exposed. This erosive action has allowed discovering a new Roman salting factory in the southern adjacent zone (Campos et al., 2015).

3. Material and methods

3.1. Field

Three sections have been studied in the meanders of the Estero de los Difuntos ebb-tide channel (Figs. 1C and 2A). These sections have been selected due to the good preservation of the sedimentary facies and their thickness in relation to other nearby sections of Saltés Island. The main features of the different sedimentary facies (granulometry, sedimentary structures, ichnology) were initially described in the field (e.g. Fig. 2C–D). Twenty-four surface sediment samples (1.5 kg dry weight) were collected for textural, mineralogical and palaeontological analyzes (Fig. 2A), being representative of the different facies observed in each section. Each sample was taken with a spatula, collected in plastic bags and labeled. Samples taken for the mineralogy were introduced in a portable cooler.

A short core (see location in Fig. 1B and stratigraphic profile in Fig. 2B) was extracted in the tidal flat of Saltés Island, in order to compare the present-day facies with the three sections mentioned above. This core was obtained with a portable vibracore (Lanesky et al., 1979) and three samples were taken according to the visual facies observed.

Two additional surface samples were collected in recent salt marshes (Fig. 1B: samples E and F). These samples were taken with a spatula, collected in plastic bags and labeled.

3.2. Laboratory

Twenty-nine subsamples (0.1 kg) were wet sieved through a sieving column ($-1 < \varphi < 4$; 2–0.063 mm) for determining the grain size distribution and the macrofaunal content of the three studied sections. Three subsamples of different facies were separated for an additional mineralogical analysis. This analysis was carried out by means of X-ray diffraction using a Philips PW 1130/90, with an automatic slit, with Kα radiation of Cu and a Ni filter at 20 Ma and 40 kv. XRD studies were carried out both on randomly oriented samples (total fraction) and selected clay fraction samples (< 2 μm). Powdered (< 63 μm) whole-rock samples were scanned from 2° to 65° 2θ. Clay fraction samples were prepared from cation-saturated, ultrasonic treated suspensions oriented on glass slides. The identification of the clay fraction minerals was carried out on oriented Mg^{2+}-saturated samples with ethylene glycol solvation, and also after heating at 550 °C following K^+ saturation. Quantitative estimation of the mineral content was carried out using the intensity factors calculated by Barahona (1974).

Additional subsamples were separated for the foraminiferal analysis. Ten grams were wet sieved (0.125 μm mesh) using distilled water and dried in an oven at 70 °C. The total population of this group present in these subsamples was analyzed and all species were determined taxonomically.

3.3. Dating

Five pristine shells of *Glycymeris* were selected for dating (Fig. 2A and Table 1). The ^{14}C method was applied by AMS at the Spanish National Centre for Accelerators (CNA), with the application of the reservoir effect correction (-108 ± 31 ^{14}C yr) calculated by Martins and Soares (2013) in this area. A mini radiocarbon dating System (MICADAS) was used. This method is based on a vacuum insulated

Table 1
Data base of ^{14}C samples and results. Reservoir effect corrected (-108 ± 31 years BP), according to Martins and Soares (2013).

LOCATION	Sample code	Laboratory code	14C age	Error	2σ calibrated age (BP)	Median probability (BP)	References
La Cascajera: central area	HU94-3	IRPA-1157	2705	90	2750–2320	2551	Dabrio et al. (2000)
La Cascajera: central area	HU94-4	IRPA-1158	2675	90	2730–2305	2521	Dabrio et al. (2000)
SECTION A	HUC-1407	CNA-2825	2170	32	2010–1765	1889	This paper
	HUCA-1406	CNA-2824	2150	33	1980–1740	1865	This paper
	HUCA-1405	CNA-2823	2172	32	2010–1770	1891	This paper
SECTION B	HUCA-1301	CNA-2817	2263	31	2120–1880	1997	This paper
SECTION C	HUCA-1401	CNA-2820	2210	32	2060–1820	1934	This paper
La Cascajera: southern area	HU94-6	UtC-4186a	1360	100	1240–800	1024	Dabrio et al. (2000)
La Cascajera: southern area	HU94-7	UtC-4187a	1300	115	1215–720	961	Dabrio et al. (2000)
La Cascajera: southern area	HU94-5	UtC-4190a	1290	105	1180–710	949	Dabrio et al. (2000)

acceleration unit that uses a commercially available 200 kV power supply to generate acceleration fields in a tandem configuration. Results are presented as calibrated ages for 2σ intervals. This method was applied to samples collected in previous investigations carried out in the Tinto-Odiel estuary to obtain a general chronological evolution of La Cascajera ridge (see Fig. 5 and Table 1).

4. Results

4.1. Facies: main sedimentary features and foraminiferal record

Five main facies have been recognized in the three sections and core D:

4.1.1. Facies 1 (poorly sorted sand)

This facies is found below the mean sea level in section C, as well as it constitutes the lower part of core D (Fig. 2A–B). Two subfacies can be distinguished: a) subfacies 1.1 (bioclastic sand), composed of shelly fine to very fine sands with numerous valves and fragments of the bivalves *Glycymeris violacescens* and *Glycymeris glycymeris* (basal samples of section C and core D); and b) subfacies 1.2 (medium to coarse yellow sand), with frequent quartz clasts and scarce fragments of mollusks (upper sample of section C). Quartz is the principal mineral of this facies (56%), with phyllosilicates as secondary components (29%). The clay mineral assemblages are dominated by illite (Fig. 3: 71%).

The foraminiferal record is diverse and abundant in subfacies 1.1 (10–21 species/sample; 100–830 individuals/10 g) and decreases remarkably in subfacies 1.2. (10 species/sample; 15 individuals/10 g). The most representative species are *Ammonia beccarii*, *Ammonia tepida*, *Elphidium advenum*, *Hanzawaia boueana*, *Neoconorbina orbicularis* and *Rosalina globularis* (Fig. 4A–B).

4.1.2. Facies 2 (bioturbated muddy sand)

This facies was observed in section A (0–0.35 m msl) and the upper part of core D. It is mainly composed of well sorted very fine sand (Fig. 3: 50–56% dry weight) with important percentages of muds (20%–31%). Quartz is the main component (56%), with lower percentages of feldspars (21%) and phyllosilicates (23%). Clay minerals are dominated by illite, but their percentages (56%) are lower than those of facies 1 (71%). Conversely, kaolinite (22%) and smectites (12%) are more abundant in facies 2.

These grayish sediments are laminated, but individual laminae are usually disturbed by bioturbation structures due to annelids, bivalves (mainly *Cerastoderma edule*) and the fiddler crab *Uca pugnax*. The base of section A includes thin sheets (< 1 cm thickness) of reddish silts and clays, near the transition to facies 3 (Fig. 2C).

Both density and diversity of the foraminiferal record are very different in the external, more exposed areas (Fig. 1B: core D) in comparison with internal, more protected zones (e.g. basal samples of section A). The sub-recent samples of core D presents a moderately abundant and diversified assemblage (Fig. 4B: 16 species/sample; 57 individuals/10 g), which is mainly composed of *A. beccarii*, *A. tepida*, *Astrononion stelligerum*, *Planorbulina mediterranensis*, *R. globularis* and several species of *Elphidium*. Nevertheless, these microorganisms are very rare in section A (Fig. 4A: 1–3 species per sample; 2–4 individuals/10 g), with very scarce individuals of *A. beccarii*, *Elphidium crispum* and *Neoeponides shreibersii*.

4.1.3. Facies 3 (bioclastic fine to coarse sand)

This facies is well represented in the three sections between the mean sea level and 1.8 m above (Fig. 2A), with a geomorphological cartography that draws a fan morphology (washover fans of Fig. 1C). These sands have two to five sequences constituted by an erosive base on facies 1 or 2, followed by lag, bioclastic deposits composed of well-sorted fine sands and numerous reworked valves of bivalves (*Glycymeris*, *Dosinia*, *Chamelea*) and gastropods (*Bittium*, *Mesalia*, *Nassarius*) with high levels of abrasion and bioerosion (Fig. 2D). The following vertical arrangement of these deposits include three main units: a) a lower unit composed of well-sorted sands (fine sand: 51–67%) with a patent planar cross-stratification northward (e.g. Fig. 2D: sample B-3); b) numerous erosive units with variable thickness (5–25 cm) and high proportions of gravel-size bioclasts (13–48% dry weight) (e.g. Fig. 2D: sample B-5); and c) medium to coarse sands with low percentages of bioclasts (< 10%) and a patent horizontal lamination (e.g. Fig. 2D: sample B-4). In most cases, individual depositional intervals display a normal grading, with micro-sequences composed of a basal, bioclastic gravel-size unit and medium to coarse sands near the top. Mineralogy of these coarse sediments is very similar to that described in facies 2, with slightly higher contents in quartz (60%) and illite as main clay mineral (Fig. 3: 73%).

Density and diversity of benthic foraminifera are greater in the basal part of this facies and the bioclastic units, whereas these microorganisms are poorly represented or can even disappear in the laminate levels (Fig. 4A). This basal lag deposits present a diverse and abundant assemblage (15–17 species; 43–123 individuals/10 g), with *A. beccarii*, *E. advenum* and *H. boueana* as most representative species. *A. beccarii* is also the main species of erosive units, together with *E. advenum* and *E. crispum*. Rare specimens of these same species were extracted from the non-bioclastic levels.

4.1.4. Facies 4 (vegetated fine to very fine sand)

This facies is observed above the mean sea level (Fig. 2A, Section C: 0.5–1.45 m msl). These fine sediments (Fig. 3: fine + very fine sand ≥50%; silt + clay: 7%–10%) constitute the recent salt marshes that overlap facies 3 (Fig. 2, section C). Dense vegetation covers these deposits, consisting of *Spartina marítima*, *Arthrocnemum* spp., *Halimione portulacoides*, *Atriplex roseus* and *Juncus maritimus* (Figueroa and Clemente, 1979). They include scattered fragments and valves of bivalves (mainly *Glycymeris* spp). Foraminifera have only been found in sample E, located in the adjacent Bacuta Island, with a scarce population composed of *Trochammina inflata* and rare specimens of *Jadammina macrescens*.

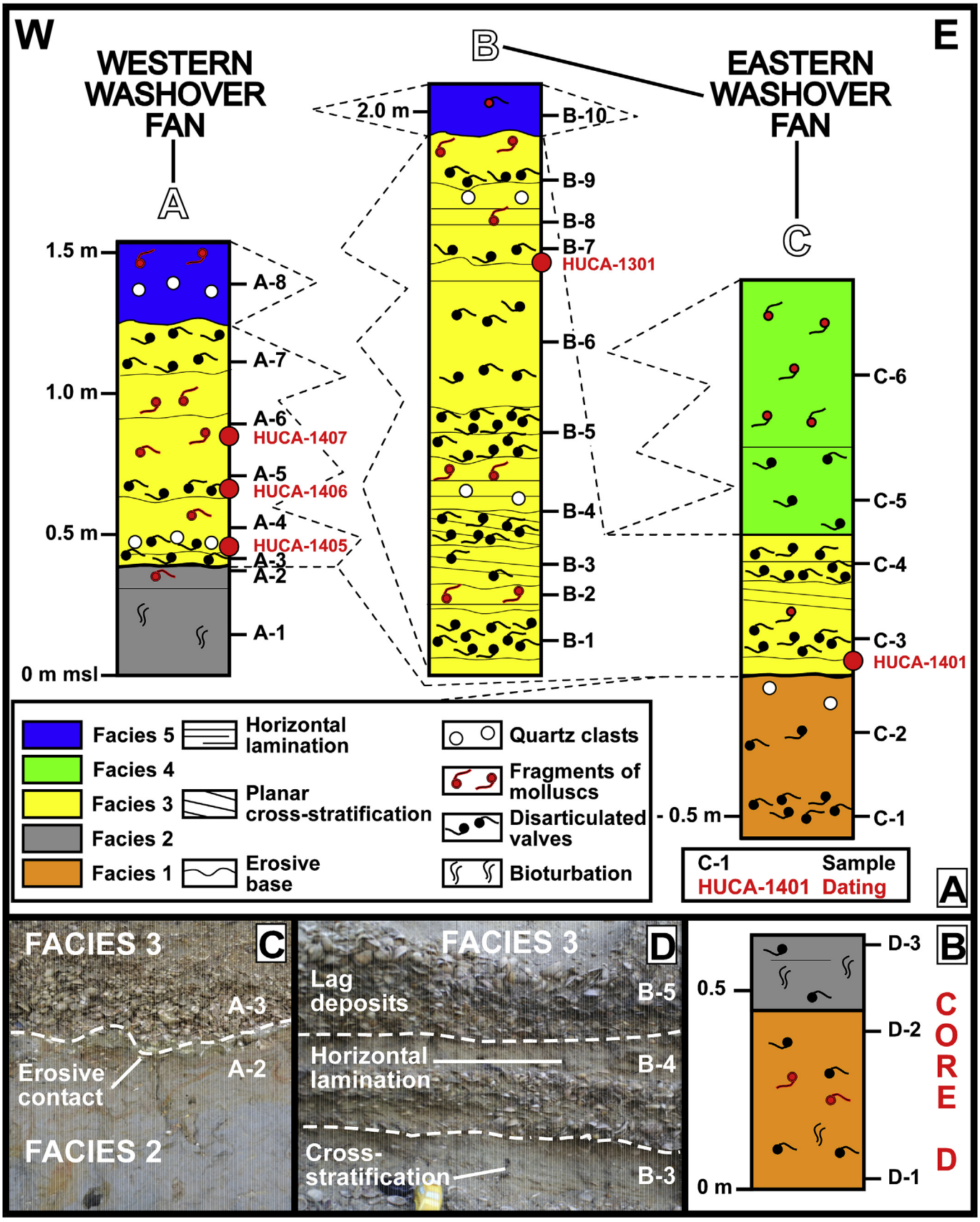

Fig. 2. A: Facies distribution and main sedimentary features, including the vertical distribution of the samples analyzed and the correlation of the studied stratigraphical logs; B: Facies distribution and samples collected in core D. C: contact between facies 2 and 3; D: Internal structure of facies 3.

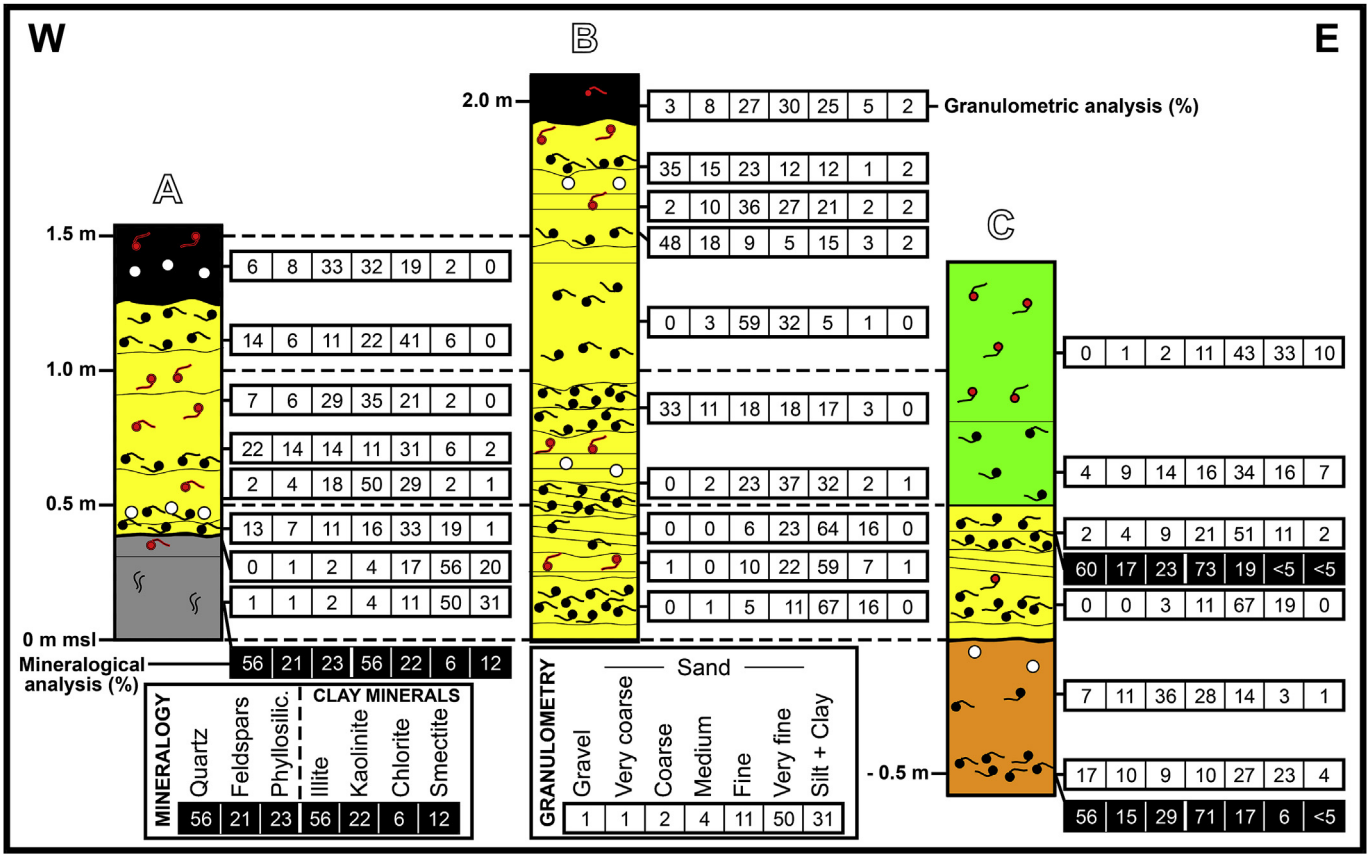

Fig. 3. Granulometric and mineralogical analysis of the samples (in wt %). Black: mineralogical analysis.

4.1.5. Facies 5 (black medium to coarse sand)

The uppermost part of sections A and B is composed of black medium to coarse sands with high organic matter contents. This level includes partially dissolved fragments of bivalves (mainly *Glycymeris* spp) and quartz clasts, while foraminifera are absent.

4.2. Chronostratigraphy

Radiocarbon chronology provides an approximation on the age of the material studied (Table 1 and Fig. 5). The five samples show very similar calibrated ages between 2120 cal yr BP and 1740 cal yr BP, although sections B and C (median probability: 1997-1934 cal yr BP) are slightly older than section A (median probability: 1891-1865 cal yr BP).

5. Discussion

5.1. Paleoenvironmental interpretation of facies

Facies 1 presents very similar features to those observed in the recent sandy tidal flat of Saltés Island (Borrego et al., 2000). The bioclastic levels are due to the landward migration of sand waves induced by tidal currents and low-energy waves (Morales et al., 2014). Decline in benthic foraminífera can be explained by the progressive decrease of the tidal immersion.

Facies 2 is interpreted as a muddy-sandy intertidal flat, with both sedimentary and biological features very similar to those described in present-day tidal flats of Saltés Island and the adjacent areas (Morales et al., 2014). In these areas, facies 2 was disposed over facies 1, with an increasing grain size (Borrego, 1992). The presence of oxidized layers in section A would be due to a prolonged subaerial exposure, a limiting factor for foraminifera that would explain its shortage in contrast with the moderate abundance of these microorganisms observed in the subrecent intertidal flat present in core D (Fig. 4B). This negative correlation between subaerial exposure and foraminiferal density has been also found in other estuaries of southwestern Spain (González-Regalado et al., 2001).

The geomorphological and sedimentological features of facies 3 are very similar to those observed in different washover fans (e.g. Barwis and Hayes, 1985; Chaumillion et al., 2017). The erosional, lag deposits are interpreted as bedload deposits, whereas the bulk of planar-stratified fine sands would have been built from deposition of suspended sediments (Shaw et al., 2015). In addition, several washovers show a basal landward dipping and upper horizontal planar laminations with numerous discontinuities, as well as individual depositional intervals with normal grading as observed in the three sections studied (Horwitz and Wang, 2005; Phantuwongraj et al., 2013). The surface cartography of this facies reveals the presence of several washover fans in the northern sector of La Cascajera (Fig. 1C). The western washover fan studied (section A) has been partially eroded by the Estero de los Difuntos ebb-tide channel, whereas sections B and C belong to a washover fan located further east (Fig. 1C).

Facies 4 constitutes the recent low salt marshes of Saltés Island. The foraminiferal record (mainly *T. inflata*) is typical of these environments in the southwestern Spanish estuaries, where foraminífera may be absent (González-Regalado et al., 2001).

Facies 5 is interpreted as an edaphic horizon coming from the weathering of washover fans. This disposition has also been observed in other stratigraphical sections of Saltés Island, in which this facies may contain Roman archaeological remains (Rodríguez Vidal et al., 2014).

5.2. Palaeoenvironmental evolution

Four phases can be defined in the palaeoenvironmental evolution of La Cascajera, based on previous research and our data. Phase I

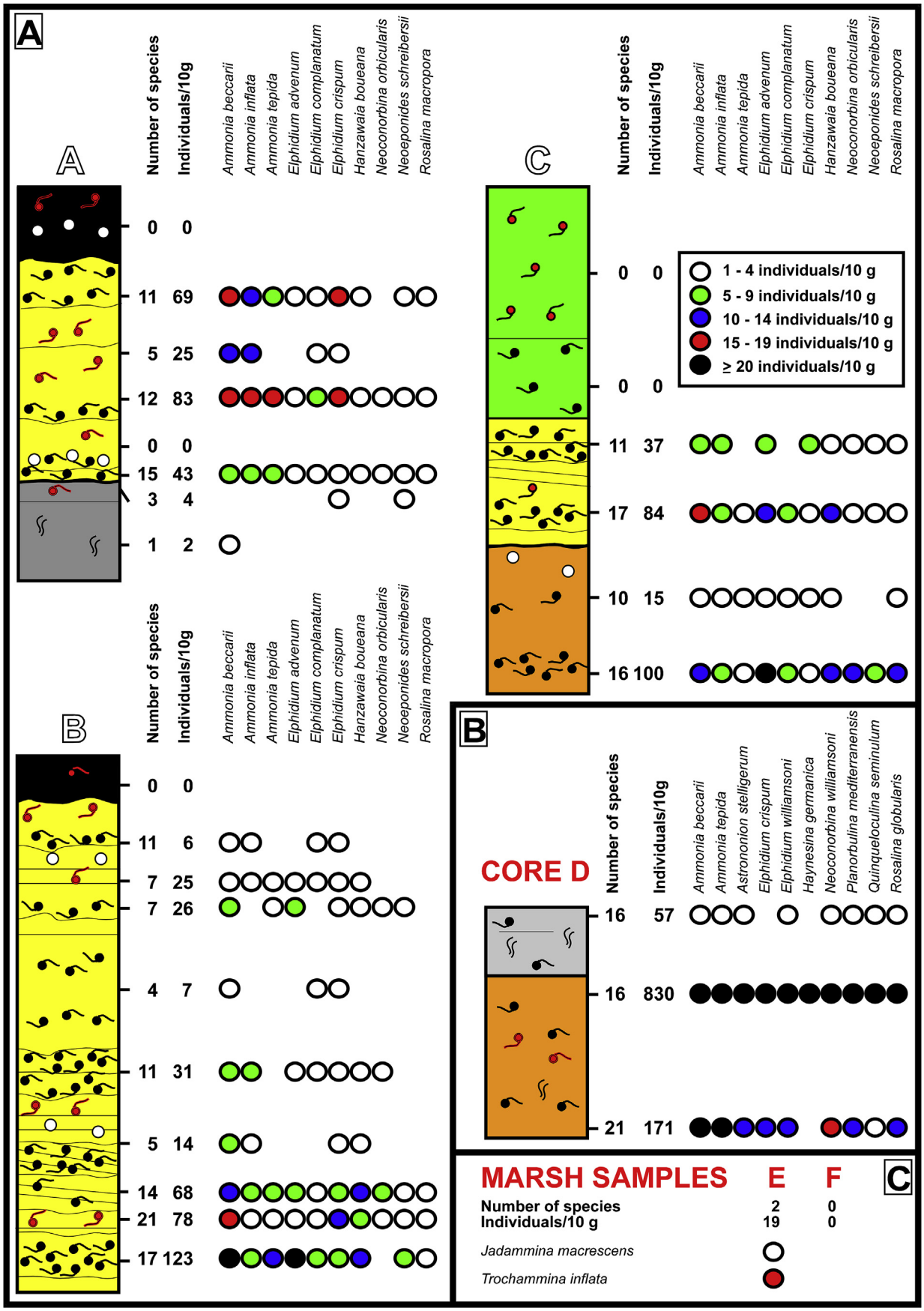

Fig. 4. Foraminifera: abundance, diversity and distribution of the main species.

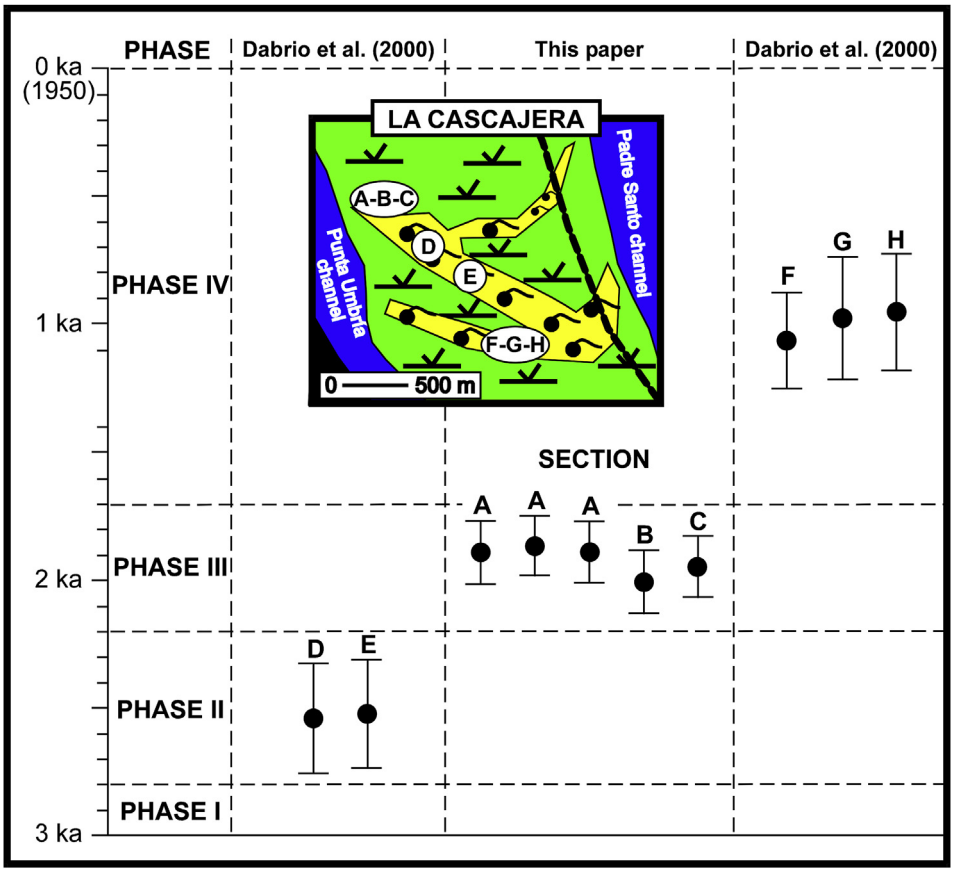

Fig. 5. Chonostratigraphy of La Cascajera (expanded from Dabrio et al., 2000).

(> 2800 cal yr BP) was characterized by the development of tidal flats in an open estuary scenario, with an initial sandy tidal plain (Fig. 6A–B: facies 1) that progressively became more clayey (facies 2) as its subaerial exposure increases (Fig. 6C–D). At present, this transition can be observed in the southern sector of Saltés Island (Figs. 1B and 2B: core D).

An important part of La Cascajera chenier was formed during Phase II (Fig. 6E–F: ~2800-2200 cal yr BP), according to datings made by Dabrio et al. (2000) in its central area (Fig. 5). Phase III (~2200-1700 cal yr BP) was defined by high-energy events that caused the formation of two washover fans (Fig. 6G–H: facies 3) in its northern part, with a partial erosion of the previous chenier and the adjacent areas. A similar age has been obtained from other high-energy deposits of Saltés Island (Campos et al., 2015).

Phase IV (1700 cal yr BP-Recent) is characterized by the development of new sandy ridges in the southwester most part of La Cascajera (Fig. 5; Dabrio et al., 2000) and the progressive emersion of new salt marshes in the central part of this area. In this phase, other adjacent cheniers emerged in this area (Fig. 1B: El Acebuchal). In the last centuries, some ebb-tide channels have eroded a part of the sedimentary sequences deposited in previous phases (Fig. 6I–J).

5.3. *The origin of washover fans*

5.3.1. *Possible hydrodynamic scenarios: regional high-energy events*

As pointed out, washover fans are usually linked to extreme wave events (see Introduction for a review). In the southwestern Spanish coast, the winter and spring storms can generate large waves (height > 7 m) and cause strong geomorphological changes in the coastal zone, such as beach erosion, recoil of dune systems, creation of new beach ridges in the main spits or even the rupture of previous cheniers and sandy spits (Rodríguez Vidal, 1987). The most probable periodicity between two high-energy periods varies between 9 and 10 years, whereas a storm period (October–April) can include more than a dozen storms (Ruiz et al., 2005b). The geological record of these storms has been detected even in internal sectors of this estuary for more than 5000 years (Ruiz et al., 2007). Consequently, these high-energy events are able to generate washover fans in this area.

Historical tsunamis are other possible causes of these deposits. Nevertheless, these tsunamigenic deposits are usually shelly beds with very limited thickness (< 30 cm in most cases), whereas facies 2 (e.g. washover fans) reaches almost 2 m thick in section B (Fig. 2). Facies 3 is constituted for two to five sequences, whereas the tsunamigenic sheets present usually a single sedimentary bed (Ruiz et al., 2004, 2005b). In general, the number of lamina sets is higher in storm deposits (Morton et al., 2007). Other tsunamigenic features such as the presence of high percentages of broken microfossils or rip-up clasts were no found in facies 3 (Dawson and Shi. 2000). Consequently, storms would be the cause of the washover fans observed in the northeastern part of La Cascajera/e.g. facies 3).

This period of high hydrodynamic instability (2100 cal yr BP-1900 cal yr BP) by high-energy events is confirmed in the Doñana National Park, located about 50 km southeast of the studied area. In the southwestern part of this Biosphere Reserve, Ruiz et al. (2004) described the deposit of marine sediments derived from high-energy events on previous salt marshes or the bottom of a lagoon, with very similar ages to facies 3.

5.3.2. *Sedimentary source*

The multidisciplinary analysis (granulometry, palaeontology, mineralogy) of washover fans allows an approximation to the sedimentary sources of these deposits. Both granulometric and macrofaunal record are very similar to those described in La Cascajera chenier, composed of medium to very coarse sands with a high bioclastic content (Morales

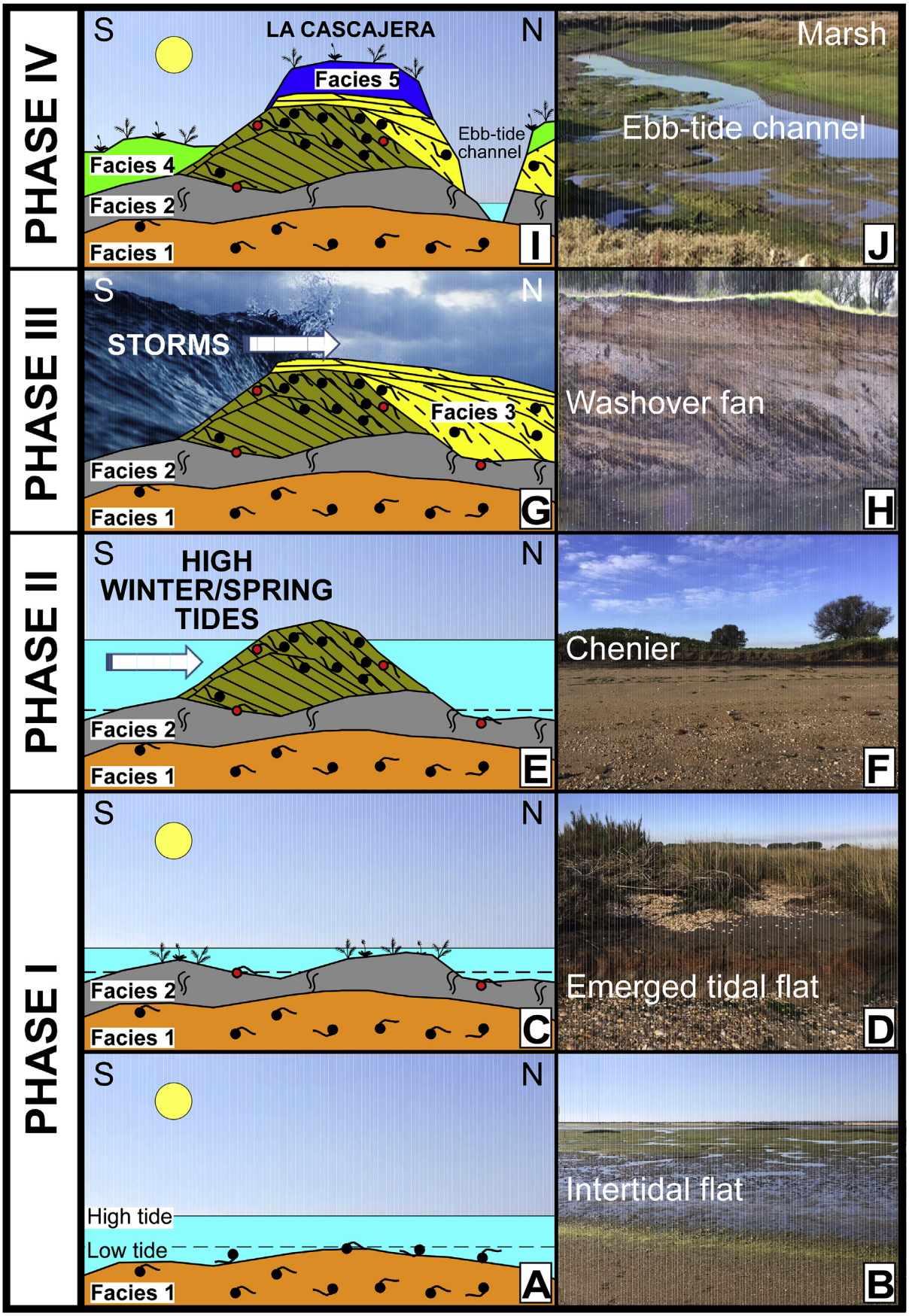

Fig. 6. Geological evolution of the northern part of La Cascajera (see text for explanation).

et al., 2014). Bioclasts of both chenier and washover fans are very similar, with numerous valves of the same bivalves (*Glycymeris glycymeris*, *G. violacescens, Dosinia lupinus*) and gastropods (*Bittium reticulatum*, *Nassarius incrassatus*) as main constituents (Gómez et al., 2016). In addition, the foraminiferal record indicates an initial tidal flat origin for washover fans (e.g. core D), with cheniers as an intermediate phase. This evolution confirms the deductions of Morales et al. (2014) about the origin of these structures.

6. Conclusions

In the Tinto-Odiel estuary, the multidisciplinary analysis of three Holocene sections, a drill core and additional surface samples permits to reconstruct the palaeoenvironmental evolution of La Cascajera ridge (Saltés Island) and the adjacent areas. Five facies were recognized, from an initial sandy tidal flat (2800 cal yr BP) to the present-day scenario. In this chenier plain, a period of high hydrodynamic instability (2100-1900 cal yr BP) caused the erosion of previous cheniers and the deposit of two washover fans owing to the action of storms. The sedimentary origin of washover fans is linked to the erosion of the La Cascajera chenier due to these events.

Acknowledgments

This work has been carried out through the projects ´Roman cities of the Baetica. CORPVS VRBIVM BAETICARVM (I) (CUB)´ (Andalusian Gouvernement) and ´From the Atlantic to the Tyrrhenian. The hispanic ports and their commercial relations with Ostia Antica. DEATLANTIR II - HAR2017-89154-P - (Plan Nacional de I + D + i). Other funds have come from Andalusian Gouvernement (groups HUM-132, RNM-238 and RNM-293). It is a contribution to the Research Center in Historical, Cultural and Natural Heritage (CIPHCN) of the University of Huelva. The authors would like to thank the helpful comments of Dr. Daria Nikitina (West Chester University) and two anonymous reviewers.

References

Atwater, B.F., Brink, U.S., Buckley, M., Halley, R.S., Jaffe, B.E., López-Venegas, A.M., Reinhard, E.G., Tuttle, M.P., Watt, S., Wei, Y., 2012. Geomorphic and stratigraphic evidence for an unusual tsunami or storm a few centuries ago at Anegada, British Virgin Islands. Nat. Hazards 63, 51–84.

Augustinus, P.G.E.F., 1989. Cheniers and cheniers plains: a general introduction. Mar. Geol. 90, 219–229.

Barahona, E., 1974. Arcillas de ladrillería de la provincia de Granada: evaluación de algunos ensayos de materias primas. Ph.D. Thesis. Granada University, Granada.

Barwis, J.H., Hayes, M.O., 1985. Antidunes on modern and ancient washover fans. J. Sed. Petrol. 55, 907–916.

Benoit, A., Sahagian, D., Carpenter, S.J., González, L.A., Frappier, B.R., 2007. Stalagmite stable isotope record of recent tropical cyclone events. Geology 35, 111–114.

Borja, F., Zazo, C., Dabrio, C.J., Dıaz del Olmo, F., Goy, J.L., Lario, J., 1999. Holocene aeolian phases and human settlements along the Atlantic coast of southern Spain. Holocene 9, 337–339.

Borrego, J., 1992. Sedimentología del estuario del río Odiel (SO España). Unpublished Ph.D. thesis (unpublished). University of Sevilla, Sevilla.

Borrego, J., Morales, J.A., Pendón, J.G., 1993. Holocene filling of an estuarine lagoon along the mesotidal coast of Huelva: the piedras river mouth, southwestern Spain. J. Coast Res. 9, 242–254.

Borrego, J., Morales, J.A., Gil, N., 2000. Evolución sedimentaria reciente de la desembocadura de la ría de Huelva. Rev. Soc. Geol. Espana 13, 405–416.

Braun, E., Meyer, B., Deocampo, D., Kiage, L.M., 2017. A 3000 yr paleostorm record from St. Catherines Island, Georgia. Estuar. Coast Shelf Sci. 196, 360–372.

Bregy, J.C., Wallace, D.J., Totten, R., Cruz, V.J., 2018. 2500-year paleotempestological record of intense storms for the northern Gulf of Mexico, United States. Mar. Geol. 396, 26–42.

Brill, D., May, S.M., Engel, M., Reyes, M., Pint, A., Opitz, S., Dierick, M., Gonzalo, L.A., Esser, S., Bruckner, H., 2016. Typhoon Haiyan's sedimentary record in coastal environments of the Philippines and its palaeotempestological implications. Nat. Hazards Earth Syst. Sci. 16, 2799–2822.

Campos, J.M., Bermejo, J., Rodríguez Vidal, J., 2015. La ocupación del litoral onubense en época romana y su relación con eventos marinos de alta energía. Cuat. Geomorfol. 29, 75–93.

Chaumillion, E., Bertin, X., Fortunato, A.B., Bajo, M., Schneider, J.-L., Dezilaeau, L., Walsh, J.P., Michelot, A., Chauveau, E., Créach, A., Hénaff, A., Sauzeau, T., Waeles, B., Gervais, B., Gwenaële, J., Baumann, J., Breilh, J.-F., Pedreros, R., 2017. Storm-induced marine flooding: lessons from a multidisciplinary approach. Quat. Sci. Rev. 165, 151–184.

Clague, J.J., Bobrowsky, P.T., Hamilton, T.S., 1994. A sand sheet deposited by the 1964 Alaska tsunami at port alberni, British columbia. Estuar. Coast Shelf Sci. 38, 413–421.

Clemmensen, L.B., Glad, A.C., Kroon, A., 2016. Storm flood impacts along the shores of micro-tidal inland seas: a morphological and sedimentological study of the Vesterlyng beach, the Belt Sea, Denmark. Geomorphology 253, 251–261.

Costas, S., Muñoz, C., Alejo, I., Pérez-Arlucea, M., 2009. Holocene evolution of a rock-bounded barrier lagoon system, Cíes Islands, northwest Iberia Holocene evolution of a rock-bounded barrier-lagoon system. Earth Surf. Proc. Landforms 34, 1575–1586.

Dabrio, C.J., Goy, J.L., Lario, J., Zazo, C., Borja, F., Gonzalez, A., 1995. The guadalete estuary during the Holocene times bay of cadiz, Spain. Int. Union Quat. Res., Subcommis. Mediterr. Black Sea Shorelines Newslett. 17, 19–22.

Dabrio, C.J., Zazo, C., Goy, J.L., Sierro, F.J., Borja, F., Lario, J., González, J.A., Flores, J.A., 2000. Depositional history of estuarine infill during the last postglacial transgression (Gulf of Cadiz, Southern Spain). Mar. Geol. 162, 381–404.

Davidson, R.G.D., Fisher, J.D., 1992. Spatial and temporal controls on overwash occurrence on a Great Lakes barrier spit. Can. J. Earth Sci. 29, 102–117.

Dawson, A., Shi, S., 2000. Tsunami deposits. Pure Appl. Geophys. 157, 875–897.

Donnelly, J.P., Butler, J., Roll, S., Wengren, M., Webb, T., 2004. A blackbarrier overwash record of intense storms from Brigantine, New Jersey. Mar. Geol. 210, 107–121.

Duck, R.W., Da Silva, J.F., 2012. Coastal lagoons and their evolution: a hydromorphological perspective. Estuar. Coast Shelf Sci. 110, 2–14.

Erikson, L.H., Espejo, A., Barnard, P.L., Serafin, K.A., Hegermiller, C.A., O´Neill, A.O., Ruggiero, P., Limber, P.W., Mendez, F.J., 2018. Identification of storm events and contiguous coastal sections for determining modeling of coastal flood events in response to climate change. Coast Eng. 140, 316–330.

Figueroa, M.E., Clemente, L., 1979. Dinámica geomorfológica de estuario de los ríos Tinto y Odiel (Huelva). Aplicación a la ordenación del territorio. Actas IV Reun. Grupo Trabajo del Cuaternario, Bañolas, pp. 79–95.

Fletcher, C.S., Rambaldi, A.N., McAllister, R.R.J., 2016. Economic, equitable, and effordable adaptations to protect coastal settlements against storm surge inundation. Reg. Environ. Change 16, 1023–1034.

Font, E., Veiga-Pires, C., Pozo, M., Nave, S., Costa, S., Ruiz, F., Abad, M., Simoes, N., Duarte, S., Rodríguez Vidal, J., 2013. Benchmarks and sediment source(s) of the 1755 Lisbon tsunami deposit at Boca do Rio Estuary. Mar. Geol. 343, 1–14.

Fuller, I.C., Macklin, M.G., Toonen, W.H.J., Holt, K.A., 2018. Storm-generated Holocene and historical fllods in the manawatu river, New Zealand. Geomorphology 310, 102–124.

Galbis, R.J., 1932. Catálogo sísmico de la zona comprendida entre los meridianos 5° E y 20° W de Greenwich y los paralelos 45° y 25º N. Dirección General del Instituto Geográfico Catastral y de Estadística, Madrid, pp. 807.

Galbis, R.J., 1940. Catálogo sísmico de la zona comprendida entre los meridianos 5° E y 20° W de Greenwich y los paralelos 45° y 25º N. Dirección General del Instituto Geográfico. Catastral y de Estadística, Madrid, pp. 277.

García-Artola, A., Stéphan, P., Cearreta, A., Kopp, R.E., Khan, N.S., Horton, B.P., 2017. Holocene sea-level database from the Atlantic coast of Europe. Quat. Sci. Rev. 196, 177–192.

Gomez, M., Humphries, M.S., Kirsten, K.L., Green, A.N., Finch, J.M., De Lecea, A.M., 2017. Diatom-inferred hydrological changes and Holocene geomorphic transitioning of Africa's largest estuarine system, Lake St Lucia. Estuar. Coast Shelf Sci. 192, 170–180.

Gómez, P., Rodríguez Vidal, J., González-Regalado, M.L., Cáceres, L.M., Toscano, A., Clemente, M.J., Redondo, A., Ruiz, F., Abad, M., Izquierdo, T., 2016. Modelo de emersión de barreras estuarinas por secuencias tempestíticas en la desembocadura de los ríos Tinto y Odiel (Huelva). Geotemas 16, 379–382.

González, F.I., Geist, E.L., Jaffe, B., Kanoglu, U., Mofjeld, H., Synolakis, C.E., Titov, V.V., Arcas, D., Bellomo, D., Carlton, D., Horning, T., Johnson, J., Newman, J., Parsons, T., Peters, R., Peterson, C., Priest, G., Venturato, A., Weber, J., Wong, F., Yalciner, A., 2009. Probabilistic tsunami hazard assessment at Seaside, Oregon, for near- and far-field seismic sources. J. Geophys. Res.: Oceans 114, c11.

González-Regalado, M.L., Ruiz, F., Baceta, J.I., González-Regalado, E., Muñoz, J.M., 2001. Total benthic foraminifera assemblages in the southwestern Spanish estuaries. Geobios 34, 39–51.

Goy, J.L., Zazo, C., Dabrio, C.J., Lario, J., Borja, F., Sierro, F.J., Flores, J.A., 1996. Global and regional factors controlling changes of coastlines in southern Iberia Spain during the Holocene. Quat. Sci. Rev. 15, 773–780.

Goy, J.L., Zazo, C., Dabrio, C.J., Baena, J., Harvey, A.M., Silva, P., Gonzalez, F., Lario, J., 1998. Sea level and climate changes in the Cabo de Gata Lagoon Almerıa during the last 6500 yr BP. Int. Union Quat. Res., Subcommis. Mediterr. Black Sea Shorelines Newslett. 20, 11–18.

Granier, B., Boichard, R., 2017. Sedimentological investigation on Holocene deposits in the mussafah channel (abu dhabi, United Arab Emirates). Carnets Géol. 17, 39–104.

Gutiérrez-Más, J.M., 2011. Glycymeris shell accumulations as indicators of recent sea-level changes and high-energy events in Cadiz Bay (SW Spain). Estuar. Coast Shelf Sci. 92, 546–554.

Hippensteel, S.P., Martin, R.E., 2000. Foraminifera of storm-generated washover fans - implications for determining storm frequency in relation to sediment supply and barrier island evolution, Folly Island, South Carolina. Envir. Micropal. 15, 351–369.

Hippensteel, S.P., Eastin, M.D., García, W.J., 2013. The geological legacy of Hurricane Irene: implications for the fidelity of the paleo-storm record. GSA Today 23, 4–10.

Horwitz, M., Wang, P., 2005. Sedimentological characteristics and internal architecture of two overwash fans from hurricanes Ivan and Jeanne. Gulf Coast Ass. Geol. Soc. Transl. 55, 342–352.

Hudock, J.W., Flaig, P.P., Wood, L.J., 2014. Washover fans: a modern geomorphologic analysis and proposed classification scheme to improve reservoir models. J. Sed. Res.

84, 854–865.
Lanesky, D.E., Logan, B.W., Brown, R.G., Hine, A.C., 1979. A new approach to portable vibracoring underwater and on land. J. Sed. Petrol. 39, 655–657.
Lario, J., Luque, L., Zazo, C., Goy, J.L., Spencer, C., Cabero, A., Bardají, T., Borja, F., Dabrio, C.J., Civis, J., González-Delgado, J.A., Borja, C., Alonso-Azcárate, J., 2010. Tsunami vs. storm surge deposits: a review of the sedimentological and geomorphological records of extreme wave events (Ewe) during the Holocene in the Gulf of Cádiz, Spain. Zeits. fur Geomorphol. 54, 301–316.
Lario, J., Zazo, C., Goy, J.L., Silva, P.G., Bardaji, T., Cabero, A., Dabrio, C.J., 2011. Holocene palaeotsunami catalogue of SW Iberia. Quat. Int. 242, 196–200.
Ledesma-Vázquez, J., Johnson, M.E., Backus, D.H., Mirabal-Davila, C., 2007. Evolución costera de un depósito de barrera transgresivo a terraza marina en Isla Coronados, Baja California Sur, México. Cienc. Mar. 33, 335–351.
Martin, A.J., Rindsberg, A.K., 2011. Ichnological diagnosis of ancient storm-washover fans, yellow banks bluff, st. Catherines island. Anthropol. Pap. Am. Mus. Nat. Hist. 94, 111–128.
Martins, J.M.M., Soares, A.M.M., 2013. Marine radiocarbon reservoir effect in Southern Atlantic Iberian coast. Radiocarbon 55, 1123–1134.
May, S.M., Brill, D., Leopold, M., Callow, J.N., Engel, M., Scheffers, A., Opitz, S., Norpoth, M., Bruckner, H., 2017. Chronostratigraphy and geomorphology of washover fans in the Exmouth Gulf (NW Australia) - a record of tropical cyclone activity during the late Holocene. Quat. Sci. Rev. 169, 65–84.
Miguel, L.L.A.J, Nehama, F.P.J., Castro, J.W.A., (in press). Lagoon-barrier system response to recent climate conditions and sea level rise, Mozambique, Africa. Estuar. Coast Shelf Sci.
Monecke, K., Finger, W., Klarer, D., Kongko, W., McAdoo, B.G., Moore, A.L., Sudrajat, S.U., 2008. A 1,000-year sediment record of tsunami recurrence in northern Sumatra. Nature 455, 1232–1234.
Morales, J.A., Borrego, J., Davies, R.A., 2014. A new mechanism for chenier development and a facies model of the Saltés Island chenier plain (SW Spain). Geomorphology 204, 265–276.
Morton, R.A., Sallenger, A.H., 2003. Morphological impacts of extreme storms barriers. J. Coast Res. 19, 560–573.
Morton, R.A., Gelfenbaum, G., Jaffe, B.E., 2007. Physical criteria for distinguishing sandy tsunami and storm deposits using modern examples. Sed. Geol. 200, 184–207.
Nikitina, D.L., Kemp, A.C., Horton, B.P., Vane, C.H., Van de Plassche, O., Engelhart, S.E., 2014. Storm erosion during the plast 2000 years along the north shore of Delaware Bay, USA. Geomorphology 208, 160–172.
Ojeda, J., 1988. Aplicaciones de la teledeteccion espacial a la dinámica litoral (Huelva). Geomorfologia y Ordenacion del Territorio. Unpublished Ph. thesis. Univ. Sevilla, Sevilla.
Otvos, E.G., Price, W.A., 1979. Problems of chenier genesis and terminology: an overview. Mar. Geol. 31, 251–263.
Pendón, J.G., 1999. La costa de Huelva. Universidad de Huelva, Huelva.
Phantuwongraj, S., Choowong, M., Nanayama, F., Hisada, K.I., Charusiri, P., Chutakositkanon, V., Pailoplee, S., Chabangbon, A., 2013. Coastal geomorphic conditions and styles of storm surge washover deposits from Southern Thailand. Geomorphology 192, 43–58.
Pilarczyk, J.E., Dura, T., Horton, B.P., Engelhart, S.E., Kemp, A.C., Sawai, Y., 2014. Microfossils as from coastal environments as indicators of paleo-earthquakes, tsunamis and storms. Palaeogeogr. Palaeoclimatol. Palaeoecol. 413, 144–157.
Pile, J., Gouramanis, C., Switzer, A.D., Rush, B., Reynolds, I., Soria, J.L.A., 2018. Can the risk of coastal hazards be better communicated. Int. J. Disaster Risk Pred. 27, 439–450.
Price, W.A., 1947. Equilibrium of form and process in tidal basins of coast of Texas and Louisiana. Am. Assoc. Petrol. Geol. Bull. 3, 1619–1663.
Ramírez-Herrera, M.T., Lagos, M., Hutchinson, I., Kostoglodov, V., Machain, M.L., Caballero, M., Goguitchaichvili, A., Aguilar, B., Chagué-Goff, C., Goff, J., Ruiz-Fernández, A.C., Ortiz, M., Nava, H., Bautista, F., López, G.I., Quintana, P., 2012. Extreme wave deposits on the Pacific coast of Mexico: tsunamis or storms-A multiproxy approach. Geomorphology 139–140, 360–371.
Rodríguez, A.B., Fegley, S.R., Ridge, J.T., VanDusen, B.M., Anderson, N., 2013. Contribution of aeolian sand to backbarrier marsh sedimentation. Estuar. Coast Shelf Sci. 117, 248–259.
Rodríguez Vidal, J., 1987. Modelo de evolución geomorfológica de la flecha litoral de Punta Umbría, Huelva, España. Cuat. Geomorfol. 1, 247–256.
Rodríguez Vidal, J., Ruiz, F., Cáceres, L.M., Abad, M., González-Regalado, M.L., Pozo, M., Carretero, M.I., Monge, A.M., Gómez, F., 2011. A. Geomarkers of the 218-209 BC atlantic tsunami in the roman *lacus ligustinus* (SW Spain): a palaeogeographical approach. Quat. Int. 242, 201–212.
Rodríguez Vidal, J., Cáceres, L.M., Abad, M., Ruiz, F., González-Regalado, M.L., Finlayson, C., Fynlayson, G., Fa, D., Rodríguez-Llanes, J.M., Bailey, G., 2011b. The recorded evidence of AD 1755 Atlantic tsunami on the Gibraltar coast. J. Iber. Geol. 37, 177–193.
Rodríguez Vidal, J., Abad, M., Cáceres, L.M., González-Regalado, M.L., Clemente, M.J., Ruiz, F., Izquierdo, T., Toscano, A., Gómez, P., Campos, J., Bermejo, J., Martínez, A., 2014. Relleno morfosedimentario y poblamiento humano del estuario de los ríos Tinto y Odiel (Huelva) durante la segunda mitad del Holoceno. In: Schnabel, S., Gómez, A. (Eds.), Avances de la Geomorfología en España 2012-2014. Sociedad Española de Geomorfología, Cáceres, pp. 604–607.
Rubio, J.C., 1985. Ecología de las marismas del Odiel. Unpublished PhD. thesis. Universidad de Sevilla, Sevilla.
Ruiz, F., Rodríguez Ramírez, A., Cáceres, L.M., Rodríguez Vidal, J., Carretero, M.I., Clemente, L., Muñoz, J.M., Yañez, C., Abad, M., 2004. Late Holocene evolution of the southwestern Doñana nacional Park (guadalquivir estuary, SW Spain): a multivariate approach. Palaeogeogr. Palaeoclimatol. Palaeoecol. 204, 47–64.
Ruiz, F., González-Regalado, M.L., Pendón, J.G., Abad, M., Olías, M., Muñoz, J.M., 2005a. Correlation between foraminifera and sedimentary environments in recent estuaries of Southwestern Spain: applications to Holocene reconstructions. Quat. Int. 140–141, 21–36.
Ruiz, F., Abad, M., Rodríguez-Ramírez, A., Cáceres, L.M., Rodríguez Vidal, J., Pino, R., Muñoz, J.M., 2005b. A statistical approach to the critical storm period analysis. In: Lehr, J. (Ed.), The Water Enciclopedia. John Wiley & Sons, New York, pp. 1–5.
Ruiz, F., Rodríguez-Ramírez, A., Cáceres, L.M., Rodríguez Vidal, J., Carretero, M.I., Abad, M., Olías, M., Pozo, M., 2005c. Evidence of high-energy events in the geological record: mid-Holocene evolution of the southwestern Doñana National Park (SW Spain). Palaeogeogr. Palaeoclimatol. Palaeoecol. 229, 212–229.
Ruiz, F., Borrego, J., López-González, N., Abad, M., González-Regalado, M.L., Carro, B., Pendón, J.G., 2007. The geological record of a Mid-Holocene marine storm in southwestern Spain. Geobios 40, 689–699.
Ruiz, F., Abad, M., Cáceres, L.M., Rodríguez Vidal, J., Carretero, M.I., Pozo, M., González-Regalado, M.L., 2010. Ostracods as tsunami tracers in Holocene sequences. Quat. Res. 73, 130–135.
Ruiz, F., Rodríguez Vidal, J., Abad, M., Cáceres, L.M., Carretero, M.I., Pozo, M., Rodríguez-Llanes, J.M., Gómez-Toscano, F., Izquierdo, T., Font, E., Toscano, A., 2013. Sedimentological and geomorphological imprints of Holocene tsunamis in Southwestern Spain: an approach to establish the recurrence period. Geomorphology 203, 97–104.
Sabatier, P., 2009. Reconstitution des évènements climatiques extrêmes (crues et tempêtes) au cours de l'Holocène dans le Golfe d'Aigues-Mortes (Sud de la France). Ph.D. thesis. University of Montpellier II, Montpellier.
Schwartz, R.K., 1982. Bedform and stratification characteristics of some modern small-scale washover sand bodies. Sedimentology 29, 835–849.
Schneider, B., Hoffmann, G., Falkenroth, M., Grade, J., (in press). Tsunami and storm sediments in Oman: characterizing extreme wave deposits using terrestrial laser scanning. J. Coast Conserv..
Shaw, J., Mohrig, D., Kocurek, G., 2015. Tracking hurricane-generated wurge with washover fan stratigraphy. Geology 43, 127–130.
Sedgwick, P.E., Davis Jr., R.A., 2003. Stratigraphy of washover fans in Florida: implications for recognition in the stratigraphic record. Mar. Geol. 200, 31–48.
Switzer, A.D., Mamo, B.L., Dominey-Howes, D., Strotz, L.C., Courtney, C., Jones, B.G., Haslett, S.K., Everett, D.M., 2011. On the possible origins of an unusual (mid to late Holocene) coastal deposit, old punt bay, south-east Australia. Geogr. Res. 49, 408–430.
Wainwright, D.J., Ranasinghe, R., Callaghan, D.P., Woodroffe, C.D., Jongejan, R., Dougherty, A.J., Rogers, K., Cowell, P.J., 2015. Moving from deterministic towards probabilistic coastal hazard and risk assessment: development of a modeling framework and application to Narrabeen Neach, New South Wales, Australia. Coast Eng. 96, 92–99.
Willershauser, T., Vott, A., Hadler, H., Ntageretzis, K., Emde, K., Bruckner, H., 2015. Holocene palaeotsunami imprints in the stratigraphical record and the coastal geomorphology of the Gialova Lagoon near Pylos (southwestern Peloponnese, Greece). Z. Geomorphol. 59, 215–252.